*Inorg. Chem.* **2007**, *46*, 8988–8997


# Synthesis and Structural Characterization of Complexes of a DO3A-Conjugated Triphenylphosphonium Cation with Diagnostically Important Metal Ions

**Chang-Tong Yang,[†] Yongxin Li,[‡] and Shuang Liu*[,†]**

*School of Health Sciences, Purdue University, West Lafayette, Indiana 47907, and School of Physical and Mathematical Sciences, Nanyang Technological University, Singapore*

Received May 29, 2007

To understand the coordination chemistry of a DO3A-conjugated triphenylphosphonium (TPP) cation, triphenyl(4-((4,7,10-tris(carboxymethyl)-1,4,7,10-tetraazacyclododecan-1-yl)methyl)benzyl)phosphonium (DO3A-xy-TPP), with diagnostically important metal ions, In(DO3A-xy-TPP)$^+$, Ga(DO3A-xy-TPP)$^+$, and Mn(DO3A-xy-TPP) were prepared by reacting DO3A-xy-TPP with 1 equiv of the respective metal salt. All three complexes have been characterized by elemental analysis, IR, ESI-MS, NMR methods (for In(DO3A-xy-TPP)$^+$ and Ga(DO3A-xy-TPP)$^+$), and X-ray crystallography. Results from HPLC concordance experiments show that $^{111}$In(DO3A-xy-TPP)$^+$ and In(DO3A-xy-TPP)$^+$ have the same composition. The solid-state structures of In(DO3A-xy-TPP)$^+$ and Mn(DO3A-xy-TPP) are very similar with DO3A being heptadentate in bonding to In(III) and Mn(II) in a monocapped octahedral coordination geometry. Because of the smaller size of Ga(III), the DO3A in Ga(DO3A-xy-TPP)$^+$ is only hexadentate with four amine-N and two carboxylate-O atoms bonding to Ga(III). One carboxylic acid group in DO3A is deprotonated to balance the positive charge of Ga(III). The coordination geometry of Ga(DO3A-xy-TPP)$^+$ is best described as a distorted octahedron. The NMR data shows that the coordinated DO3A in In(DO3A-xy-TPP)$^+$ and Ga(DO3A-xy-TPP)$^+$ is symmetrical in aqueous solution. There is no dissociation of the acetate chelating arms in In(DO3A-xy-TPP)$^+$ and Ga(DO3A-xy-TPP)$^+$, providing indirect evidence for the high solution stability of $^{111}$In(DO3A-xy-TPP)$^+$ and $^{68}$Ga(DO3A-xy-TPP)$^+$.

## Introduction

Alteration in the electric component or mitochondrial membrane potential ($\Delta\Psi_m$) is an important characteristic of cancer caused directly by mitochondrial dysfunction, such as DNA mutation and oxidative stress.[1−4] It has been reported that the mitochondrial transmembrane potential in carcinoma cells is significantly higher than that in normal epithelial cells.[5−9] For example, the difference in $\Delta\Psi_m$ between the CX-1 colon carcinoma cells and the control green monkey kidney epithelial cell line was approximately 60 mV (163 mV in tumor cells vs 104 mV in normal cells). The observation that the enhanced mitochondrial transmembrane potential is prevalent in the tumor-cell phenotype provides the conceptual basis for development of mitochondrial-targeting diagnostic and therapeutic pharmaceuticals.[1−3,10−13]

Measurement of mitochondrial transmembrane potential ($\Delta\Psi_m$) provides the most comprehensive reflection of

* To whom correspondence should be addressed. Phone: 765-494-0236. Fax: 765-496-1377. E-mail: lius@pharmacy.purdue.edu.
[†] Purdue University.
[‡] Nanyang Technological University.

(1) Kroemer, G.; Dallaporta, B.; Resche-Rigon, M. *Annu. Rev. Physiol.* **1998**, *60*, 619−642.
(2) Modica-Napolitano, J. S.; Aprille, J. R. *Adv. Drug Delivery Rev.* **2001**, *49*, 63−70.
(3) Duchen, M. R. *Mol. Aspects Med.* **2004**, *25*, 365−451.
(4) Modica-Napolitano, J. S.; Singh, K. K. *Expert Rev. Mol. Med.* **2002**, (02)00445-3a, http://www.ermm.cbcu.cam.ac.uk (short code: txt001ksb).
(5) Johnson, L. V.; Walsh, M. L.; Chen, L. B. *Proc. Natl. Acad. Sci. U.S.A.* **1980**, *77*, 990−994.
(6) Summerhayes, I. C.; Lampidis, T. J.; Bernal, S. D.; Nadakavukaren, J. J.; Nadakavukaren, K. K.; Shepard, E. L.; Chen, L. B. *Proc. Natl. Acad. Sci. U.S.A.* **1982**, *79*, 5292−5296.
(7) Modica-Napolitano, J. S.; Aprille, J. R. *Cancer Res.* **1987**, *47*, 4361−4365.
(8) Davis, S.; Weiss, M. J.; Wong, J. R.; Lampidis, T. J.; Chen, L. B. *J. Biol. Chem.* **1985**, *260*, 3844−3850.
(9) Dairkee, S. H.; Hackett, A. J. *Breast Cancer Res. Treat.* **1991**, *18*, 57−61.
(10) Gottlieb, E.; Thompson, C. B. *Methods Mol. Biol.* **2003**, *223*, 543−554.
(11) Mannella, C. A. *Biochim. Biophys. Acta* **2006**, *1762*, 140−147.
(12) Ross, M. F.; Kelso, G. F.; Blaikie, F. H.; James, A. M.; Cocheme, H. M.; Filipovska, A.; Da Ros, T. D.; Hurd, T. R.; Smith, R. A. J.; Murphy, M. P. *Biochemistry (Moscow)* **2005**, *70*, 222−230.



10.1021/ic7010452 CCC: $37.00 
Published on Web 09/05/2007

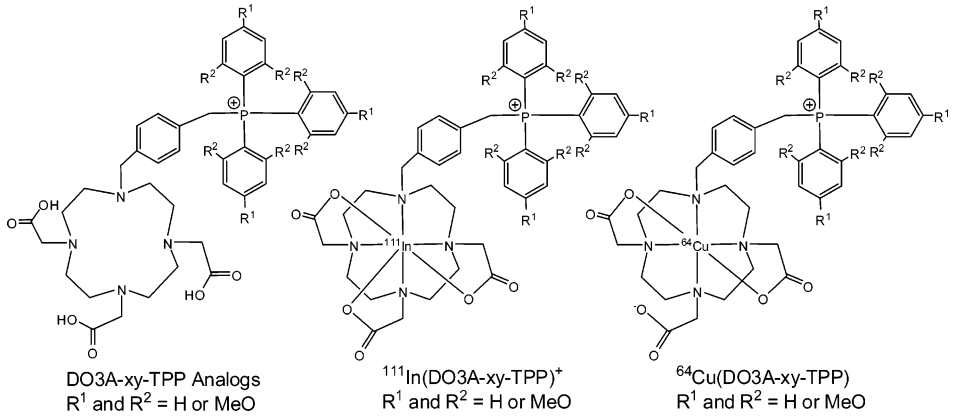


**Figure 1.** DO3A-conjugated TPP analogs and their radiometal complexes useful for imaging tumors.

mitochondrial bioenergetic function primarily because it depends directly on proper integration of diverse metabolic pathways that converge at mitochondria. Because plasma and mitochondrial transmembrane potentials are negative, delocalized cationic molecules with appropriate structural features are driven electrophoretically through these membranes and tend to accumulate inside the energized mitochondria.[1−4,11] For example, lipophilic cations, such as rhodamine-123 and $^{3}$H-tetraphenylphosphonium ($^{3}$H-TPP), have been widely used to measure mitochondrial potentials in tumor cells.[1,14−16] According to the Nernst equation, the 60 mV difference in $\Delta\Psi_m$ between carcinoma and control epithelial cell is theoretically sufficient to account for a 10-fold greater accumulation of cationic compounds in carcinoma mitochondria than in those of normal cells.[1−4,11] In addition, the plasma membrane potential (30−90 mV) also preconcentrates the cationic species relative to the external medium, thus affecting the cytoplasmic concentration of these compounds and their availability for mitochondrial uptake.

Recently, several groups reported the use of radiolabeled triphenylphosphonium (TPP) cations, such as 4-($^{18}$F-benzyl)-triphenylphosphonium (Figure 1, $^{18}$F-BzTPP), as positron-emission tomography (PET) potential radiotracers for tumor and heart imaging.[17−25] Even though $^{3}$H-tetraphenylphosphonium (Figure 1, $^{3}$H-TPP) was reported to have a better tumor uptake than $^{99m}$Tc-Sestamibi, its tumor selectivity is very poor with the tumor/heart ratio being <0.2.[19,23] In addition, $^{3}$H-TPP is not suitable for imaging purposes. The high uptake of $^{18}$F-BzTPP in the heart and liver may also impose a significant challenge for its clinical applications in the diagnosis of cancer in the chest and abdominal regions. Thus, there is an urgent need for new radiotracers that have high tumor selectivity and are able to provide information of mitochondrial bioenergetic function in tumors by monitoring mitochondrial potential in a noninvasive fashion.

Previously, we reported several $^{64}$Cu-labeled triphenylphosphonium (TPP) cations, such as $^{64}$Cu(DO3A-xy-TPP) (Figure 1, DO3A-xy-TPP = triphenyl(4-((4,7,10-tris(carboxymethyl)-1,4,7,10-tetraazacyclododecan-1-yl)methyl)benzyl)phosphonium), as new radiotracers for imaging tumors by positron-emission tomography (PET).[26] The TPP moiety acts as the "mitochondrion-targeting biomolecule" to carry $^{64}$Cu into tumor cells.[26] DO3A is used as the bifunctional chelator because it is able to form highly stable radiometal chelates with radionuclides, such as $^{64}$Cu and $^{68}$Ga for PET, $^{111}$In for single-photon emission computed tomography (SPECT), and $^{90}$Y and $^{177}$Lu for radiotherapy. Biodistribution and microPET imaging studies have demonstrated that the $^{64}$Cu-labeled TPP cations are able to localize in tumors with high tumor uptake (2−3.5% ID/g) and high tumor selectivity (tumor/heart ratio $\approx$ 5:1 at 2 h postinjection, as compared to tumor/heart ratio being <0.2 during the 2 h study period for $^{99m}$Tc-Sestamibi). The high tumor selectivity of the $^{64}$Cu-labeled TPP cations is related to their low lipophilicity.[26] The in vitro assay data show that $^{64}$Cu(DO3A-xy-TPP) is able to localize in mitochondria of U87MG glioma cells. The $^{111}$In-labeled TPP cations also have high tumor uptake, but their tumor selectivity is not as good as that of their $^{64}$Cu analogs.[27]

In our previous report,[26] we described the synthesis of Cu(DO3A-xy-TPP) as part of the characterization of $^{64}$Cu-labeled TPP cations. However, we were not able to obtain crystals of Cu(DO3A-xy-TPP) suitable for structural determination by X-ray crystallography. To understand the coordination chemistry of DO3A-conjugated TPP cations

(13) Jakobs, S. *Biochim. Biophys. Acta* **2006**, *1763*, 561−575.
(14) Lichtshtein, D.; Kaback, H. R.; Blume, A. J. *Proc. Natl. Acad. Sci. U.S.A.* **1979**, *76*, 650−654.
(15) Hockings, P. D.; Rogers, P. J. *Biochim. Biophys. Acta* **1996**, *1282*, 101−106.
(16) Huang, S. G. *J. Biomol. Screening* **2002**, *7*, 383−389.
(17) Krause, B. J.; Szabo, Z.; Becker, L. C.; Dannals, R. F.; Scheffel, U.; Seki, C.; Ravert, H. T.; Dipaola, A. F., Jr.; Wagner, H. N., Jr. *J. Nucl. Biol. Med.* **1994**, *38*, 521−526.
(18) Madar, I.; Anderson, J. H.; Szabo, Z.; Scheffel, U.; Kao, P. F.; Ravert, H. T.; Dannals, R. F. *J. Nucl. Med.* **1999**, *40*, 1180−1185.
(19) Madar, I.; Weiss, L.; Izbicki, G. *J. Nucl. Med.* **2002**, *43*, 234−238.
(20) Ravert, H. T.; Madar, I.; Dannals, R. F. *J. Label. Compd. Radiopharm.* **2004**, *47*, 469−476.
(21) Madar, I.; Ravert, H. T.; Du, Y.; Hilton, J.; Volokh, L.; Dannals, R. F.; Frost, J. J.; Hare, J. M. *J. Nucl. Med.* **2006**, *47*, 1359−1366.
(22) Cheng, Z.; Subbarayan, M.; Chen, X.; Gambhir, S. S. *J. Label. Compd. Radiopharm.* **2005**, *48*, 131−137.
(23) Min, J. J.; Biswal, S.; Deroose, C.; Gambhir, S. S. *J. Nucl. Med.* **2004**, *45*, 636−643.
(24) Steichen, J. D.; Weiss, M. J.; Elmaleh, D. R.; Martuza, R. L. *J. Neurosurg.* **1991**, *74*, 116−122.
(25) Cheng, Z.; Winant, R. C.; Gambhir, S. S. *J. Nucl. Med.* **2005**, *46*, 878−886.
(26) Wang, J.; Yang, C.-T.; Kim, Y.-S.; Sreerama, S. G.; Chen, X.; Liu, S. *J. Med. Chem.* In press.
(27) Kim, Y.-S.; Yang, C.-T.; Wang, J.; Sreerama, S. G.; Chen, X.; He, Z.; Liu, S. Unpublished work.

with diagnostically important metals and the impact of radiometal chelates on biological properties of the radiolabeled TPP cations, we prepared In(III), Ga(III), and Mn(II) complexes of DO3A-xy-TPP. We are interested in the Ga(III) and In(III) complexes because of their potential applications as PET ($^{68}$Ga) and SPECT ($^{67}$Ga and $^{111}$In) radiotracers. The Mn(II) complex is particularly interesting because of its potential as a magnetic resonance imaging (MRI) contrast agent and its similarity to its Cu(II) analog with respect to molecular charge. In this report, we present the synthesis and structural characterization of M(DO3A-xy-TPP)$^+$ (M = Ga and In) and Mn(DO3A-xy-TPP). The main objective of this study is to determine their structures in both the solid state and solution. Biodistribution and imaging data for $^{64}$Cu-labeled TPP cations has been described previously.[26] Biological evaluation for the $^{111}$In-labeled TPP cations will be reported as a separate account.[27]

## Experimental Section

**Materials and Instruments.** Chemicals were obtained from Sigma/Aldrich (St. Louis, MO). 1,4,7,10-Tetraazacyclododecane-4,7,10-tris(*t*-butyl acetate) (DO3A(OBu-t)$_3$) was purchased from Macrocyclics Inc. (Dallas, TX). NMR ($^1$H, $^{13}$C, $^{31}$P, $^1$H-$^1$H COSY, HMQC, HSQC, HMBC, and NOESY) data were obtained using Bruker DRX 300 MHz and Bruker Avance 500 MHz FT NMR spectrometers. Chemical shifts are reported in parts per million (ppm) relative to TMS. Infrared (IR) spectra were recorded on a Perkin-Elmer FT-IR spectrometer. Mass spectra were collected using positive mode on a Finnigan LCQ classic mass spectrometer, School of Pharmacy, Purdue University. Elemental analysis was performed by Dr. H. Daniel Lee using a Perkin-Elmer Series III analyzer, Department of Chemistry, Purdue University.

**HPLC Method.** The HPLC method used a UV−vis detector ($\lambda$ = 254 nm), a $\beta$-ram IN-US detector, and a Zorbax Rx-C18 column (4.6 mm × 150 mm, 300 Å pore size). The flow rate was 1 mL/min with the mobile phase being isocratic with 80% solvent A (10 mM ammonium acetate) and 20% solvent B (acetonitrile) at 0−5 min, followed by a gradient mobile phase going from 20% B at 5 min to 60% B at 20 min.

**In(DO3A-xy-TPP)(OAc).** DO3A-xy-TPP was prepared according to the procedure described in our previous report.[26] DO3A-xy-TPP (71.1 mg, 0.1 mmol) and In(OAc)$_3$ (29.1 mg, 0.1 mmol) were dissolved in 0.2 mL of $NH_4OAc$ buffer (0.5 M, pH = 6.0). The mixture was stirred and heated at 100 °C for 30 min. After filtration, the filtrate was transferred into a clean 5 mL vial. Slow diffusion of acetone into the reaction mixture produced colorless crystals suitable for X-ray crystallography. The solid was separated by filtration and dried under vacuum overnight before being submitted for elemental analysis. The yield was 52.2 mg (~63.5%). A sample was analyzed by HPLC. The HPLC retention time was 14.7 min with a purity of >95%. IR (cm$^{-1}$, KBr pellet): 1629.6 (s, $\nu_{C=O}$), 3435.2 (bs, $\nu_{O-H}$). ESI-MS: $m/z$ = 823.16 for $[M + H]^+$ (823.60 calcd for $[C_{40}H_{45}InN_4O_6P]^+$). The $^1$H and $^{13}$C NMR data are listed in Table 1. $^{31}$P NMR ($D_2O$, 500 Hz, 25 °C): $\delta$ 19.5 (s, 1P). Anal. Calcd for $C_{42}H_{48}InN_4O_8P\cdot(CH_3)_2CO\cdot3H_2O$: C, 54.32; H, 6.03; N, 5.63. Found: C, 54.68; H, 6.19; N, 5.76.

**Ga(DO3A-xy-TPP)(NO$_3$).** Ga(DO3A-xy-TPP)(NO$_3$) was prepared using $Ga(NO_3)_3\cdot H_2O$ (27.3 mg, 0.1 mmol) according to the same procedure for In(DO3A-xy-TPP)(OAc). Slow diffusion of acetone into the reaction mixture produced colorless crystals suitable for X-ray crystallography. The solid was separated and dried under vacuum overnight before being submitted for elemental analysis. The yield was 64.4 mg (~67.6%). The HPLC retention time was 14.8 min with a purity of >95%. IR (cm$^{-1}$, KBr pellet): $\delta$ 1632.7 (s, $\nu_{C=O}$), 1726.6 (s, $\nu_{C=O}$), 3441.3 (bs, $\nu_{O-H}$). ESI-MS: $m/z$ = 777.02 for $[M + H]^+$ (778.50 calcd for $[C_{40}H_{45}GaN_4O_6P]^+$). $^1$H and $^{13}$C NMR data are listed in Table 1. $^{31}$P NMR ($D_2O$, 300 Hz, 25 °C): $\delta$ 26.3 (s, 1P). Anal. Calcd For $C_{40}H_{46}GaN_5O_9\cdot(CH_3)_2CO\cdot3H_2O$: C, 54.16; H, 6.06; N, 7.35. Found: C, 54.42; H, 5.93; N, 7.02.

**Mn(DO3A-xy-TPP).** Mn(DO3A-xy-TPP) was prepared using $MnCl_2$ (12.5 mg, 0.1 mmol) according to the same procedure for In(DO3A-xy-TPP)(OAc). Slow diffusion of methanol into the reaction mixture afforded colorless crystals suitable for X-ray crystallography. The solid was separated and dried under vacuum before being submitted for elemental analysis. The yield was 61.7 mg (~71.2%). A sample was analyzed by HPLC. The retention time was 16.8 min with a purity of >95%. IR (cm$^{-1}$, KBr pellet): 1637.1 (s, $\nu_{C=O}$), 3429.3 (bs, $\nu_{O-H}$). ESI-MS: $m/z$ = 764.09 for $[M + H]^+$ (763.72 calcd for $[C_{40}H_{45}MnN_4O_6P]$). Anal. Calcd for $C_{40}H_{45}MnN_4O_6P\cdot4H_2O\cdot CH_3OH$: C, 54.46; H, 7.03; N, 5.72. Found: C, 54.24; H, 6.71; N, 5.70.

**$^{111}$In(DO3A-xy-TPP)$^+$.** $NH_4OAc$ buffer (0.5 mL, 0.1 M, pH 6.9) containing 50 $\mu$g of the DO3A-xy-TPP and 0.10 mL of $^{111}InCl_3$ solution (0.2−2.0 mCi) in 0.05 N HCl were added to a clean 3 mL plastic vial. The mixture was heated at 100 °C for 30 min. After the mixture was cooled to room temperature, a sample of the resulting solution was analyzed by radio-HPLC. The HPLC retention time was 14.7 min. The HPLC concordance experiment was performed by injection of the HPLC-purified $^{111}$In(DO3A-xy-TPP)$^+$ and In(DO3A-xy-TPP)$^+$ sequentially under the same chromatographic conditions.

**X-ray Crystallographic Analysis.** Crystallographic data for In(DO3A-xy-TPP)(OAc)·7.5H$_2$O·(CH$_3$)$_2$CO, Ga(DO3A-xy-TPP)(NO$_3$)·6H$_2$O·(CH$_3$)$_2$CO, and Mn(DO3A-xy-TPP)·4H$_2$O·CH$_3$OH were collected on a Nonius Kappa CCD diffractometer and are listed in Table 2. Crystals were mounted on a glass fiber in a random orientation. Preliminary examination and data collection were performed using graphite-monochromated Mo K$\alpha$ radiation ($\lambda$ = 0.71073 Å). Cell constants for data collection were obtained from least-squares refinement, using the setting angles of 23 636 reflections in the range of $2 < \lambda < 25°$ for In(DO3A-xy-TPP)(OAc)·7.5H$_2$O·(CH$_3$)$_2$CO. A total of 23 636 reflections were collected, and 9031 reflections were unique. Lorentz and polarization corrections were applied to the data. The linear absorption coefficient is 5.6 cm$^{-1}$ for Mo K$\alpha$ radiation. An empirical absorption correction using SCALEPACK[28] was applied. The structure was solved by direct methods using Charge Flipping[29] in PLUTON.[30] There are eight oxygen atom positions of water molecules found in In(DO3A-xy-TPP)(OAc)·7.5H$_2$O·(CH$_3$)$_2$CO, seven of which have full occupancies, while one has fractional occupancy. For Ga(DO3A-xy-TPP)(NO$_3$)·6H$_2$O·(CH$_3$)$_2$CO, cell constants for data collection were obtained from least-squares refinement, using the setting angles of 18 858 reflections in the range of $3 < \lambda < 27°$. The refined mosaicity from DENZO/SCALEPACK[28] was 0.34°, indicating good crystal quality. A total of 18 858 reflections were collected, of which 8697 were unique. Frames were integrated with DENZO-SMN.[28] Lorentz and polarization corrections were applied to the data. The linear absorption coefficient is 7.0 cm$^{-1}$ for Mo K$\alpha$ radiation. An empirical absorption correction using SCALEPACK[28] was applied.

(28) Otwinowski, Z.; Minor, W. *Methods Enzymol.* **1997**, *276*, 307.
(29) Oszlanyi, G.; Suto, A. *Acta Crystallogr.* **2004**, *A60*, 134.
(30) Spek, A. L. *PLATON, Molecular Graphics Program;* University of Utrecht: Utrecht, The Netherlands, 1991.

**Table 1.** $^{1}H$ and $^{13}C$ NMR Data (500 Hz) for In(DO3A-xy-TPP)$^{+}$ and Ga(DO3A-xy-TPP)$^{+}$[a]

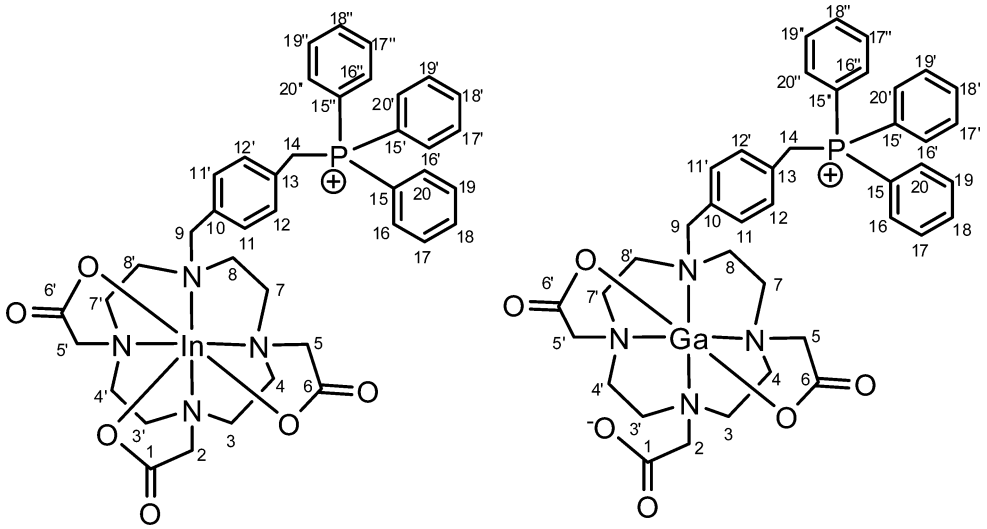


| | In(DO3A-xy-TPP)$^{+}$ | | Ga(DO3A-xy-TPP)$^{+}$ | |
|---|---|---|---|---|
| position | $\delta_H$ (mult., $J_{HH}$) | $\delta_C$ | $\delta_H$ (mult., $J_{HH}$) | $\delta_C$ |
| 1 | | 178.2 | | 173.1 |
| 2 | 3.53 (s) | 60.1 | 3.54 (s) | 62.5 |
| 3, 3′ | 3.09 (m), 3.33 (m) | 54.8 | 3.26 (m), 4.02 (m) | 53.8 |
| 4, 4′ | 3.04 (m), 3.25 (m) | 54.8 | 3.35 (m), 3.51 (m) | 56.2 |
| 5, 5′ | 3.62 (AB quartet) | 61.5 | 3.85 (AB quartet) | 58.7 |
| 6, 6′ | | 177.9 | | 173.0 |
| 7, 7′ | 3.04 (m), 3.29 (m) | 53.5 | 3.35 (m), 3.51 (m) | 56.5 |
| 8, 8′ | 2.69 (m) | 49.1 | 2.89 (m), 3.39 (m) | 53.3 |
| 9 | 3.96 (s) | 58.9 | 3.92 (s) | 63.5 |
| 10 | | 132.6 | | 129.9 |
| 11, 11′ | 7.11 (d, 9.8 Hz) | 134.9 | 7.20 (d, 9.8 Hz) | 131.2 |
| 12, 12′ | 7.00 (d, 9.8 Hz) | 133.7 | 6.96 (d, 9.8 Hz) | 130.5 |
| 13 | | 131.0 | | 128.2 |
| 14 | 4.78 (d, 9.8 Hz) | 31.7 (d) | 4.78 (d, 9.8 Hz) | 28.6 (d) |
| 15, 15′,15″ | | 119.7(d) | | 116.3 |
| 16, 16′, 16″ | 7.65 (m) | 136.6 | 7.57 (m) | 133.3 |
| 17, 17′, 17″ | 7.65 (m) | 132.5 | 7.57 (m) | 129.1 |
| 18, 18′, 18″ | 7.86 (t) | 137.7 | 7.78 (m) | 134.4 |
| 19, 19′, 19″ | 7.65 (m) | 132.5 | 7.57 (m) | 129.1 |
| 20, 20′, 20″ | 7.65 (m) | 136.6 | 7.57 (m) | 133.3 |

[a] Both $^{1}H$ and $^{13}C$ NMR spectra were recorded in $D_2O$ at 25 °C.

The structure was solved by direct methods using SIR2004.[31] Refinement was performed on a LINUX PC using SHELX-97.[32] There were six O atom positions of lattice water molecules found in Ga(DO3A-xy-TPP)$^{+}$. No hydrogen atom was included for these oxygen atoms, for which only the isotropic thermal parameter was refined. Crystallographic drawings were done using programs ORTEP[33] and PLUTON.[30] For Mn(DO3A-xy-TPP)·4$H_2O$·$CH_3OH$, the cell constants for data collection were obtained from least-squares refinement, using the setting angles of 26 583 reflections in the range of $2 < \lambda < 26°$. A total of 26 583 reflections were collected, and 6443 reflections were unique. Lorentz and polarization corrections were applied to the data. The linear absorption coefficient is 4.1 $cm^{-1}$ for Mo K$\alpha$ radiation. An empirical absorption correction using SCALEPACK[28] was applied. The structure was solved by direct methods using SIR2004.[31] Refinement was performed on a LINUX PC using SHELX-97.[32] Crystallographic drawings were done using programs ORTEP.[33]

## Results

**Synthesis.** In this study, we prepared Ga(DO3A-xy-TPP)$^{+}$, In(DO3A-xy-TPP)$^{+}$, and Mn(DO3A-xy-TPP) by reacting DO3A-xy-TPP with 1 equiv of the respective metal salt in 0.5 M ammonium acetate buffer (pH 6). Heating was needed to complete the reaction. Ga(DO3A-xy-TPP)$^{+}$ and In(DO3A-xy-TPP)$^{+}$ were designed as model compounds for $^{67/68}$Ga-(DO3A-xy-TPP)$^{+}$ and $^{111}$In(DO3A-xy-TPP)$^{+}$, respectively. Mn(DO3A-xy-TPP) was prepared because of its potential as a MRI contrast agent and its similarity to the Cu(II) analog with respect to molecular charge and lipophilicity.[26] Both In(DO3A-xy-TPP)$^{+}$ and Ga(DO3A-xy-TPP)$^{+}$ were isolated as the complex cations with acetate and nitrate as counterions, respectively. Mn(DO3A-xy-TPP) was obtained as the zwitterion salt. All three compounds have been characterized by IR, ESI-MS, HPLC, elemental analysis, and X-ray crystallography. In(DO3A-xy-TPP)$^{+}$ and Ga(DO3A-xy-TPP)$^{+}$ have

(31) Burla, M. C.; Caliandro, R.; Camalli, M.; Carrozzini, B.; Cascarano, G. L.; Caro, L. De; Giacovazzo, C.; Polidori, G.; Spagna, R. *J. Appl. Crystallogr.* **2005**, *38*, 381.
(32) Sheldrick, G. M. *SHELXL 97, A Program for Crystal Structure Refinement*; University of Göttingen: Göttingen, Germany, 1997.
(33) Johnson, C. K. *ORTEPII*; Report ORNL-5138; Oak Ridge National Laboratory: Oak Ridge, TN, 1976.

**Table 2.** Selected Crystallographic Data and Structure Refinements Details for In(DO3A-xy-TPP)(OAc)·7.5$H_2O$·$(CH_3)_2CO$, Ga(DO3A-xy-TPP)($NO_3$)·6$H_2O$·$(CH_3)_2CO$, and Mn(DO3A-xy-TPP)·4$H_2O$·$CH_3OH$

| | $C_{45}H_{69}InN_4O_{16.5}P$ | $C_{43}H_{64}GaN_5O_{16}P$ | $C_{41}H_{57}MnN_4O_{11}P$ |
|---|---|---|---|
| fw | 1075.83 | 1007.71 | 867.84 |
| space group | $P\bar{1}$ (No. 2) | $Pca2_1$ (No. 29) | $P2_1/c$ (No. 14) |
| $\lambda$ (Å) | Mo Kα (0.71073) | Mo Kα (0.71073) | Mo Kα (0.71073) |
| $a$ (Å) | 10.7779(9) | 28.9585(9) | 12.8899(9) |
| $b$ (Å) | 16.3040(17) | 8.15090(10) | 19.1761(10) |
| $c$ (Å) | 16.4520(18) | 19.6548(6) | 17.1960(13) |
| α (deg) | 103.482(6) | 90 | 90 |
| $\beta$ (deg) | 106.939(6) | 90 | 103.84(4) |
| $\gamma$ (deg) | 104.783(6) | 90 | 90 |
| $V$ (Å$^3$) | 2522.0(4) | 4639.3(2) | 4127.0(5) |
| $Z$ | 2 | 4 | 4 |
| $d_{calcd}$ (g/cm$^3$) | 1.417 | 1.443 | 1.397 |
| $T$ (K) | 150 | 150 | 150 |
| $\mu$ (mm$^{-1}$) | 0.572 | 0.696 | 0.406 |
| transm coeff | 0.788, 0.932 | 0.812, 0.773 | 0.954, 0.985 |
| $R(F_o)$ | 0.056[a] | 0.043[a] | 0.069[a] |
| $R_w(F_o^2)$ | 0.135[b] | 0.094[b] | 0.161[b] |

[a] $R = \sum||F_o| - |F_c||/\sum|F_o|$ for $F_o^2 > 2\sigma(F_o^2)$. [b] $R_w = [\sum w(|F_o^2| - |F_c^2|)^2/\sum w|F_o^2|^2]^{1/2}$.

also been studied by NMR spectroscopic methods ($^1$H, $^{13}$C, $^{31}$P, $^1$H-$^1$H COSY, HSQC, HMQC, HMBC, and NOESY) to determine their solution structures.

**IR and ESI-MS.** The IR spectrum of In(DO3A-xy-TPP)(OAc) shows a strong and broad band at 3435 cm$^{-1}$ attributed to $\nu_{O-H}$ of the crystallization water molecules and a strong band at 1630 cm$^{-1}$ from the coordinated carboxylate groups. Upon coordination, stretching frequencies from the carboxylic groups ($\nu_{C=O} \approx 1730$ cm$^{-1}$) undergo a significant "red-shift" ($\sim$100 cm$^{-1}$). The IR spectra of complexes Ga(DO3A-xy-TPP)($NO_3$) and Mn(DO3A-xy-TPP) also show broad bands at 3441 and 3429 cm$^{-1}$, respectively, attributed to crystallization water molecules and strong bands at 1633 cm$^{-1}$ for Ga(DO3A-xy-TPP)($NO_3$) and 1637 cm$^{-1}$ for Mn(DO3A-xy-TPP) attributed to the coordinated carboxylate groups. A strong band at 1727 cm$^{-1}$ was observed for the uncoordinated carboxylate group in Ga(DO3A-xy-TPP)($NO_3$). Two strong bands at 1300 and 1412 cm$^{-1}$ are typical of non-coordinating $NO_3^-$ counterions in Ga(DO3A-xy-TPP)($NO_3$). The ESI-MS of In(DO3A-xy-TPP)(OAc) shows a molecular ion at $m/z = 823.16$ for $[M + H]^+$, while the ESI-MS of Ga(DO3A-xy-TPP)($NO_3$) has the molecular ion at $m/z = 777.02$ for $[M + H]^+$. Mn(DO3A-xy-TPP) displays the molecular ion at $m/z = 764.09$ for $[M + H]^+$ in its ESI mass spectrum.

**HPLC Analysis.** The same HPLC method was used to determine relative lipophilicity of Ga(DO3A-xy-TPP)$^+$, In(DO3A-xy-TPP)$^+$, and Mn(DO3A-xy-TPP). Figure 2 illustrates their representative HPLC chromatograms. The presence of a single peak in the region of interest suggests that they exist in solution as a single or "averaged" species under the chromatographic conditions used in this study. The HPLC retention times for In(DO3A-xy-TPP)$^+$ and Ga(DO3A-xy-TPP)$^+$ are almost identical (14.5 and 14.7 min, respectively), but they are significantly shorter than that of

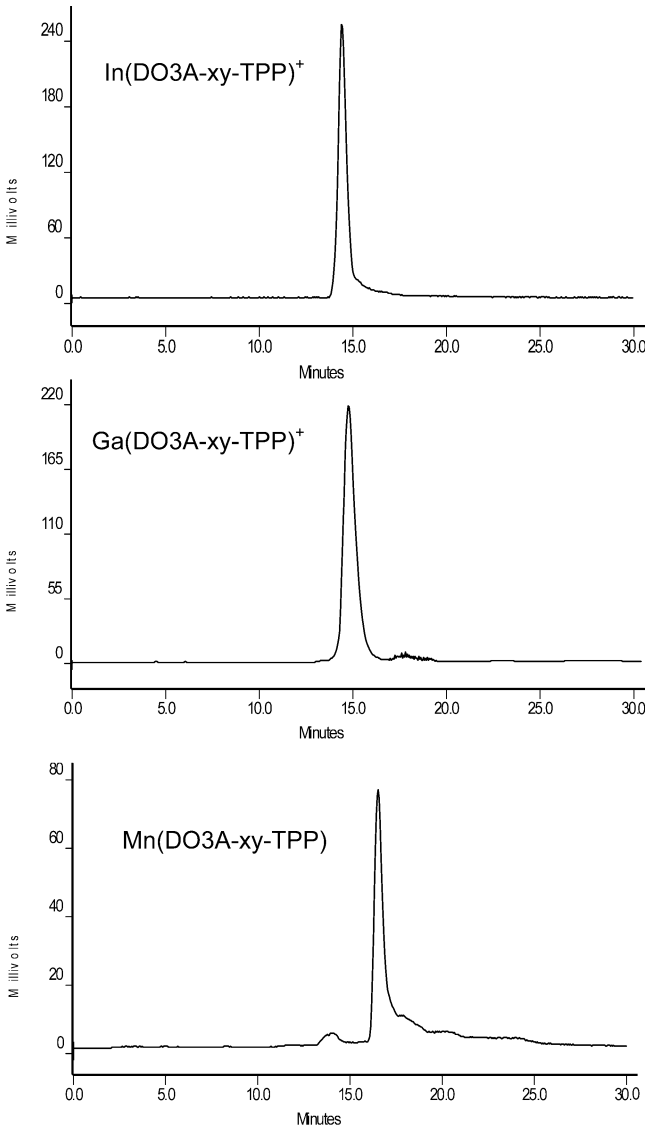


**Figure 2.** Representative HPLC chromatograms of Ga(DO3A-xy-TPP)$^+$, In(DO3A-xy-TPP)$^+$, and Mn(DO3A-xy-TPP).

Mn(DO3A-xy-TPP) (16.8 min). Obviously, Ga(DO3A-xy-TPP)$^+$ and In(DO3A-xy-TPP)$^+$ with the +1 overall molecular charge are more hydrophilic (shorter HPLC retention time) than Mn(DO3A-xy-TPP) in the zwitterion form. The HPLC retention time of Mn(DO3A-xy-TPP) is very close to that of Cu(DO3A-xy-TPP) (17.2 min) under identical chromatographic conditions.[26]

**HPLC Concordance Experiment.** The HPLC concordance experiment was performed using HPLC-purified $^{111}$In(DO3A-xy-TPP) and In(DO3A-xy-TPP). Figure 3 shows HPLC chromatograms of In(DO3A-xy-TPP)$^+$ (top) and $^{111}$In(DO3A-xy-TPP)$^+$ (bottom) under the same chromatographic conditions. Since they share almost identical HPLC retention times, we believe that $^{111}$In(DO3A-xy-TPP)$^+$ and In(DO3A-xy-TPP)$^+$ have the same composition at both tracer and macroscopic levels.

**Structure of In(DO3A-xy-TPP)$^+$.** Figure 4 illustrates an ORTEP view of In(DO3A-xy-TPP)$^+$. There are two In(DO3A-xy-TPP)(OAc) molecules in each unit cell, along with eight crystallization water molecules and one acetone

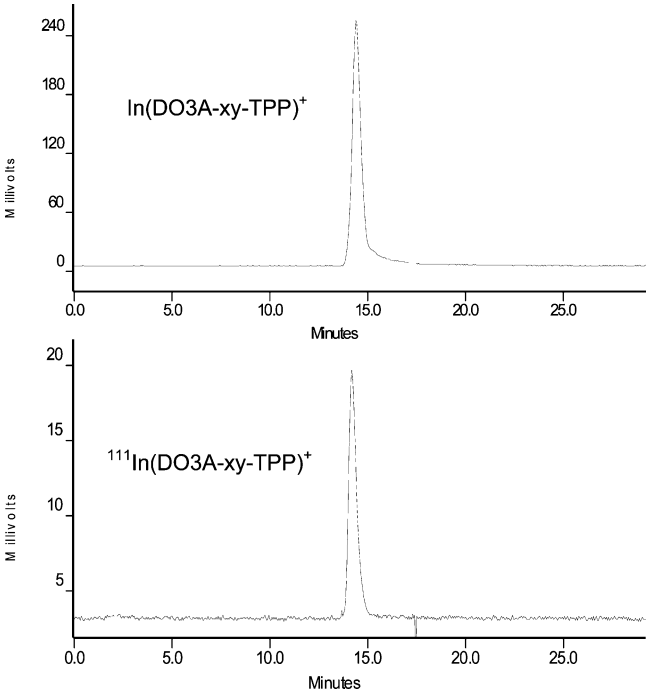


**Figure 3.** HPLC concordance for In(DO3A-xy-TPP)$^+$ (top) and $^{111}$In-(DO3A-xy-TPP)$^+$ (bottom). Their identical HPLC retention times suggest that $^{111}$In(DO3A-xy-TPP)$^+$ and In(DO3A-xy-TPP)$^+$ have the same composition.

**Table 3.** Selected Bond Distances (Å) and Bond Angles (deg) in In(DO3A-xy-TPP)(OAc)·7.5$H_2O$·$(CH_3)_2CO$

| atom 1 | atom 2 | distance |
|---|---|---|
| In51 | O41 | 2.159(3) |
| In51 | O71 | 2.162(3) |
| In51 | O101 | 2.202(3) |
| In51 | N10 | 2.327(3) |
| In51 | N1 | 2.375(3) |
| In51 | N7 | 2.395(3) |
| In51 | N4 | 2.399(3) |

| atom 1 | atom 2 | atom 3 | angle |
|---|---|---|---|
| O41 | In51 | O71 | 87.22(14) |
| O41 | In51 | O101 | 84.51(12) |
| O71 | In51 | O101 | 79.45(13) |
| O41 | In51 | N10 | 152.56(14) |
| O71 | In51 | N10 | 103.51(14) |
| O101 | In51 | N10 | 73.04(13) |
| O41 | In51 | N1 | 86.06(13) |
| O71 | In51 | N1 | 164.99(14) |
| O101 | In51 | N1 | 86.55(13) |
| N10 | In51 | N1 | 77.22(14) |
| O41 | In51 | N7 | 131.71(14) |
| O71 | In51 | N7 | 73.31(15) |
| O101 | In51 | N7 | 131.84(13) |
| N10 | In51 | N7 | 75.72(14) |
| N1 | In51 | N7 | 120.82(14) |
| O41 | In51 | N4 | 75.61(14) |
| O71 | In51 | N4 | 114.19(13) |
| O101 | In51 | N4 | 154.85(14) |
| N10 | In51 | N4 | 120.38(14) |
| N1 | In51 | N4 | 77.00(13) |
| N7 | In51 | N4 | 73.30(14) |

surrounding each In(DO3A-xy-TPP)$^+$. DO3A acts as a heptadentate ligand in bonding to In(III) with four amine-N and three carboxylate-O donor atoms. The coordination geometry in In(DO3A-xy-TPP)$^+$ is best described as a monocapped octahedron, in which there are three amine-N atoms, N(1), N(4), N(10), and three oxygen atoms, O(41), O(71), O(101), from the carboxylate groups. The atom N(7) caps the triangular face formed by N(4), N(10), and O(71). In(DO3A-xy-TPP)$^+$ has a symmetry plane that is defined by four atoms: N(1), In(51), N(7), and O(71). The structure of In(DO3A-xy-TPP)$^+$ is very similar to those of Na[In(L1)]-$(NO_3)(H_2O)(C_2H_5OH)$·2.65$H_2O$ ($H_3L1$ = tris(2′-hydroxybenzylaminoethyl)amine)[34] and [In(DO3A)]·2$H_2O$·MeOH.[35]

Table 3 lists selected In−N and In−O bond distances and selected bond angles in In(DO3A-xy-TPP)$^+$. The average In−N bond length is 2.374 Å (In(51)−N(1) = 2.375(4) Å, In(51)−N(4) = 2.399(4) Å, In(51)−N(10) = 2.327(4) Å, In(51)−N(7) = 2.395(4) Å), which is close to that (average In−N distance = 2.356 Å) of In(DO3A)·2$H_2O$·MeOH[35] and is slightly shorter than that (average In−N distance = 2.430 Å) of In(DOTA-AA) (DOTA-AA = 1,4,7,10-tetraazacyclododecane-1,4,7,10-tetraacetic acid mono(*p*-aminoanilide)) because of its smaller coordination number.[36] The average In−O bond length is 2.174 Å (In(51)−O(41) = 2.159(3) Å, In(51)−O(71) = 2.162(3) Å, and In(51)−O(101) = 2.202-(3) Å), which is comparable to that observed in In(DO3A)·2$H_2O$·MeOH (average In−O distance = 2.181 Å),[35] but it is shorter than that of In(DOTA-AA) (average In−O distance = 2.2191 Å).[36] The N(7) amine-nitrogen atom caps the triangular face formed by N(4), N(10), and O(71), leading to the enlarged triangular face (O(71)−In(51)−N(4)= 114.19-(13)°, N(10)−In(51)−N(4) = 120.38(14)°, O(71)−In(51)−N(10) = 103.51(14)°) and the reduced triangular face formed by N(1), O(41), and O(101) (O(41)−In(51)−N(1) = 86.06-(13)°, O(101)−In(51)−N(1) = 86.55(13)°, and O(41)−In-(51)−O(101) = 84.51(12)°). The In(51)−N(7) bond distance is 2.395(4) Å, which is significantly shorter than that (In-(1)−N(7) = 2.752(4) Å) in Na[In(L1)]$(NO_3)(H_2O)(C_2H_5$-OH)·2.65$H_2O$.[34]

**Structure of Ga(DO3A-xy-TPP)$^+$.** Figure 5 shows the ORTEP view of Ga(DO3A-xy-TPP)$^+$. In each unit cell, there are four Ga(DO3A-xy-TPP)$(NO_3)$ molecules, along with six crystallization water molecules and one acetone surrounding each Ga(DO3A-xy-TPP)$(NO_3)$. The coordinated DO3A is hexadentate with four amine-N and two carboxylate-O donor atoms bonding to Ga(III) due to its smaller size than that of In(III). The remaining acetic acid group is uncoordinated and deprotonated to balance the positive charge of Ga(III). The coordination geometry around the Ga(III) is best described as a distorted octahedron with N(4), N(10), O(41), and O(101) forming the equatorial plane and N(1) and N(7) occupying the remaining two axial positions. The structure of Ga(DO3A-xy-TPP)$^+$ is very similar to that reported for Ga(DOTA-D-Phe$NH_2$) (DOTA-D-Phe$NH_2$ = 1,4,7,10-tetraazacyclododecane-4,7,10-tricarboxymethyl-1-yl-acetyl-D-Phe-$NH_2$),[37] Ga(HDOTA)·5.5$H_2O$ (DOTA = 1,4,7,10-tetraazacyclododecane-4,7,10-triacetic acid),[38] [Ga(Brbad)]-

(34) Liu, S.; Rettig, S. J.; Orvig, C. *Inorg. Chem.* **1992**, *26*, 5400.
(35) Riesen, A.; Kaden, T. A.; Ritter, W.; Mäcke, H. R. *Chem. Commun.* **1989**, 460.
(36) Liu, S.; He, Z.; Hsieh, W.-Y.; Fanwick, P. E. *Inorg. Chem.* **2003**, *42*, 8831.
(37) Heppler, A.; Froidevaux, S.; Mäcke, H. R.; Jermann, E.; Béhé, M.; Powell, P.; Hennig, M. *Chem.—Eur. J.* **1999**, *5*, 1974.
(38) Viola, N. A.; Rarig, Jr., R. S.; Ouellette, W.; Doyle, R. P. *Polyhedron* **2006**, *25*, 3457.

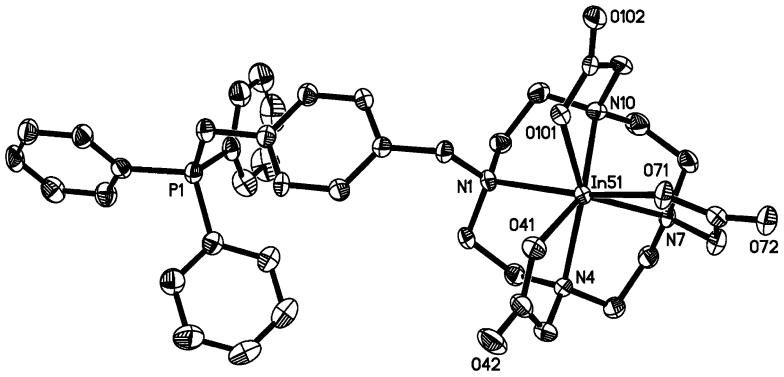


**Figure 4.** ORTEP drawing of In(DO3A-xy-TPP)$^+$. Ellipoids are at 50% probability. Crystallization molecules and hydrogen atoms are omitted for the sake of clarity.

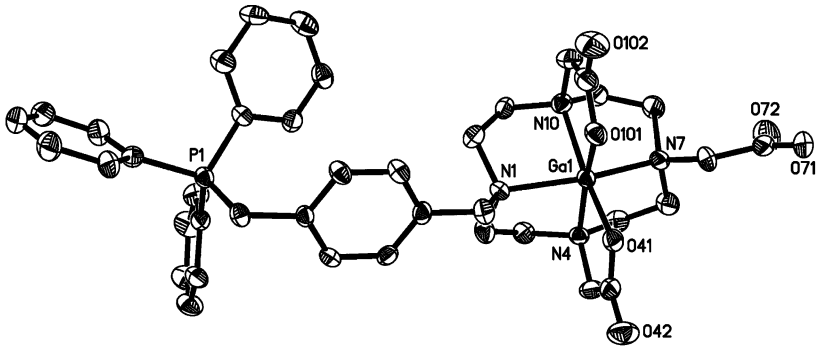


**Figure 5.** ORTEP drawing of Ga(DO3A-xy-TPP)$^+$. Ellipoids are at 50% probability. Crystallization molecules and hydrogen atoms are omitted for the sake of clarity.

$ClO_4$·DMSO ($H_2$Brbad = 1,10-bis(2-hydroxy-5-bromobenzyl)-1,4,7,10-tetraazadecane),[39] and [Ga(HL3)]Cl·$CHCl_3$ ($H_3$-L3 = tris(5′-bromo-2′-hydroxybenzylaminoethyl)amine).[34] There is a symmetry plane that is defined by N(1), Ga(1), and N(7) and that divides the coordinated DO3A moiety into two identical parts. As a result, the bond angle N(10)−Ga-(1)−N(7) (83.35(11)°) is almost identical to that of N(4)−Ga(1)−N(7) (83.52(12)°), while the bond angle N(10)−Ga(1)−N(1) (82.72(11)°) is very close to the angle N(4)−Ga(1)−N(1) (83.10(12)°).

Table 4 lists the selected bond distances and bond angles in Ga(DO3A-xy-TPP)$^+$. The average Ga−N bond length is 2.127 Å (Ga(1)−N(4) = 2.115(3) Å, Ga(1)−N(10) = 2.122-(3) Å, Ga(1)−N(7) = 2.125(3) Å, Ga(1)−N(1) = 2.147(2) Å), which is very similar to those of Ga(HDOTA)·5.5$H_2O$ (average Ga−N distance = 2.123 Å),[38] [Ga(Brbad)]$ClO_4$·DMSO (average Ga−N distance = 2.112 Å),[39] and [Ga-(HL3)]Cl·$CHCl_3$ (average Ga−N distance = 2.113 Å)[34] and is slightly shorter than that of Ga(DOTA-D-Phe$NH_2$) (average Ga−N distance = 2.141 Å).[37] The equatorial Ga−N bonds (2.125(3) and 2.147(2) Å) are slightly longer than the axial ones (2.115(3) and 2.122(3) Å). The average Ga−O bond length is 1.930 Å (Ga(1)−O(41) = 1.926(2) Å, Ga-(1)−O(101) = 1.934(3) Å), which is very close to that of Ga(HDOTA)·5.5$H_2O$ (1.935 Å)[38] and slightly longer than that of [Ga(Brbad)]$ClO_4$·DMSO (1.913 Å),[39] [Ga(HL3)]Cl·$CHCl_3$ (1.901 Å)[34], and Ga(DOTA-D-Phe$NH_2$) (1.918 Å).[37]

(39) Wong, E.; Liu, S.; Lügger, T.; Hahn, F. E.; Orvig, C. *Inorg. Chem.* **1995**, *34*, 93.

**Table 4.** Selected Bond Distances (Å) and Bond Angles (deg) in Ga(DO3A-xy-TPP)$(NO_3)$·6$H_2O$·$(CH_3)_2CO$

| atom 1 | atom 2 | distance |
|---|---|---|
| Ga1 | O41 | 1.926(2) |
| Ga1 | O101 | 1.934(3) |
| Ga1 | N4 | 2.115(3) |
| Ga1 | N10 | 2.122(3) |
| Ga1 | N7 | 2.125(3) |
| Ga1 | N1 | 2.147(2) |

| atom 1 | atom 2 | atom 3 | angle |
|---|---|---|---|
| O41 | Ga1 | O101 | 84.95(12) |
| O41 | Ga1 | N4 | 84.17(11) |
| O10 | Ga1 | N4 | 168.95(11) |
| O41 | Ga1 | N10 | 168.13(11) |
| O10 | Ga1 | N10 | 83.25(12) |
| N4 | Ga1 | N10 | 107.67(11) |
| O41 | Ga1 | N7 | 97.49(10) |
| O101 | Ga1 | N7 | 99.82(11) |
| N4 | Ga1 | N7 | 83.52(12) |
| N10 | Ga1 | N7 | 83.35(11) |
| O41 | Ga1 | N1 | 99.95(9) |
| O101 | Ga1 | N1 | 96.91(12) |
| N4 | Ga1 | N1 | 83.10(12) |
| N10 | Ga1 | N1 | 82.72(11) |
| N7 | Ga1 | N1 | 156.76(11) |

**Structure of Mn(DO3A-xy-TPP).** A representative ORTEP view of Mn(DO3A-xy-TPP) is shown in Figure 6. Crystallization water molecules and hydrogen atoms are omitted for the sake of clarity. In general, there are four Mn(DO3A-xy-TPP) molecules in each unit cell, along with four crystallization water molecules and one methanol molecule surrounding each Mn(DO3A-xy-TPP). Like that in In(DO3A-xy-TPP)$^+$, the DO3A is heptadentate with all four amine-N

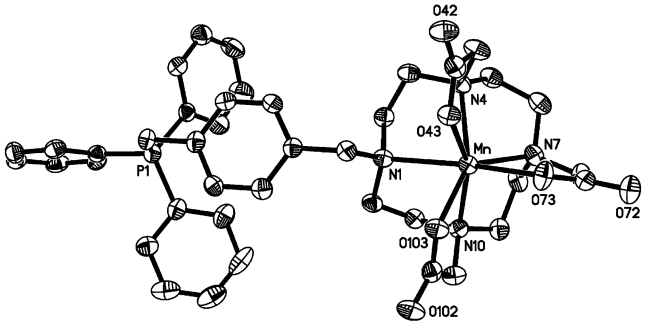


**Figure 6.** ORTEP drawing of Mn(DO3A-xy-TPP). Ellipoids are at 50% probability. Crystallization water molecules and hydrogen atoms are omitted for the sake of clarity.

**Table 5.** Selected Bond Distances (Å) and Bond Angles (deg) in Mn(DO3A-xy-TPP)·4$H_2O$·$CH_3OH$

| atom 1 | atom 2 | distance |
|---|---|---|
| Mn | O103 | 2.161(3) |
| Mn | O73 | 2.190(3) |
| Mn | O43 | 2.196(3) |
| Mn | N4 | 2.379(3) |
| Mn | N10 | 2.421(3) |
| Mn | N1 | 2.447(3) |
| Mn | N7 | 2.455(3) |

| atom 1 | atom 2 | atom 3 | angle |
|---|---|---|---|
| O103 | Mn | O73 | 89.64(11) |
| O103 | Mn | O43 | 87.98(10) |
| O73 | Mn | O43 | 84.66(11) |
| O103 | Mn | N4 | 150.19(11) |
| O73 | Mn | N4 | 110.85(12) |
| O43 | Mn | N4 | 73.29(11) |
| O103 | Mn | N10 | 74.55(11) |
| O73 | Mn | N10 | 107.81(12) |
| O43 | Mn | N10 | 158.14(11) |
| N4 | Mn | N10 | 116.45(12) |
| O103 | Mn | N1 | 82.34(11) |
| O73 | Mn | N1 | 170.65(11) |
| O43 | Mn | N1 | 90.23(11) |
| N4 | Mn | N1 | 74.94(11) |
| N10 | Mn | N1 | 74.75(11) |
| O103 | Mn | N7 | 134.40(11) |
| O73 | Mn | N7 | 71.13(11) |
| O43 | Mn | N7 | 128.75(11) |
| N4 | Mn | N7 | 74.43(11) |
| N10 | Mn | N7 | 72.98(11) |

and three carboxylate-O atoms bonding to the Mn(II). There is a symmetry plane defined by N(1), Mn, N(7), and O(71) in the coordinated DO3A. The coordination geometry of Mn(DO3A-xy-TPP) is very similar to that of In(DO3A-xy-TPP)$^+$. Three amine-N atoms, N(1), N(4), and N(10), and three carboxylate-O atoms, O(43), O(73), and O(103), form the distorted octahedron. The remaining amine-N atom, N(7), caps the triangular face formed by N(4), N(10), and O(73).

Table 5 lists selected Mn−N and Mn−O bond distances and selected bond angles in the coordination sphere of Mn(DO3A-xy-TPP). The average Mn−N bond length is 2.426 Å (Mn−N(1) = 2.447(3) Å, Mn−N(4) = 2.379(3) Å, Mn−N(10) = 2.421(3) Å, Mn−N(7) = 2.455(3) Å), which is in agreement with those previously reported.[40,41] The average Mn−O bond length is 2.182 Å (Mn−O(43) = 2.196(3) Å, Mn−O(73) = 2.190(3) Å, Mn−O(103) = 2.161(3) Å), which is slightly shorter than that of [Mn(EDTB)(Ac)](Ac)·$C_2H_5$-OH (EDTB = *N*,*N*,*N*′,*N*′-tetrakis(2′-benzimidazolylmethyl)-1,2-ethanediamine).[41] The Mn−N(7) bond distance is 2.455(3) Å with N(7) capping the triangular face formed by N(4), N(10), O(73), which leads to an increase of the triangular face (N(4)−Mn−O(73) = 110.85(12)°, N(4)−Mn−N(10) = 116.45(12)°, N(10)−Mn−O(73) = 107.81(12)°) and a decrease of the triangular face formed by N(1), O(43), and O(103) (N(1)−Mn−O(43) = 90.23(12)°, N(1)−Mn−O(103) = 82.34(11)°, O(103)−Mn−O(43) = 87.98(10)°) in the octahedron. The coordination numbers of the Mn(II) complexes range from four to eight.[44] Seven-coordinated Mn(II) complexes normally have the coordination geometry of either monocapped octahedron or a pentagonal bipyramid.[39−43,45−47]

**NMR for In(DO3A-xy-TPP)$^+$ and Ga(DO3A-xy-TPP)$^+$.** Since $^{111}$In(DO3A-xy-TPP)$^+$ and $^{67/68}$Ga(DO3A-xy-TPP)$^+$ are used as radiotracers in biological systems, it is necessary to study their solution properties (structure, isomerism, and stability) in aqueous solution. The solution structures of In(DO3A-xy-TPP)$^+$ and Ga(DO3A-xy-TPP)$^+$ were elucidated using NMR methods ($^1$H, $^{13}$C, $^1$H−$^1$H COSY, HSQC, HMQC, HMBC, and NOESY), while isomerism and stability were monitored by variable-temperature $^1$H NMR spectroscopy. Table 1 summarizes $^1$H NMR and $^{13}$C NMR data for In(DO3A-xy-TPP)$^+$ and Ga(DO3A-xy-TPP)$^+$ in $D_2O$ at 25 °C. Assignments of resonance signals from the phenyl, *p*-xylene, and acetate groups were based on results from the $^1$H−$^1$H COSY, NOESY, HSQC, and HMQC experiments at 25 °C (Figures SI−SVI). The assignment of resonance signals from protons of the cyclen backbone was tentative because many of them are superimposed.

Figure 7 shows the aliphatic region of $^1$H NMR spectra of In(DO3A-xy-TPP)$^+$ in $D_2O$ at 5 (top) and 25 °C (bottom). The doublet at 4.73 ppm is assigned to H14 and H14′ of the P*C*$H_2$$C_6H_4$ moiety. Splitting is caused by coupling from the phosphonium-P. The singlet at 3.96 ppm is from H9 and H9′ of the N*C*$H_2$$C_6H_4$ moiety. The singlet at 3.53 is from H2a and H2b in the acetate chelating arm attached to N(7). The AB quartet at ∼3.6 ppm is assigned to H5a, H5b, H5a′, and H5b′ of the two opposite acetate chelating arms. The multiplets at 3.33 and 3.09 ppm are tentatively assigned to H3a, H3a′, H3b, and H3b′ of the macrocycle. The multiplets at 3.25 and 3.04 ppm are most likely from eight methylene protons (H4, H4′, H7, and H7′), while the broad peak at 2.69 ppm is probably from the other methylene protons (H8a,

(40) Luo, Y.; Zhang, J.; Lu, L.; Qian, M.; Wang, X.; Yang, X. *Transition Met. Chem.* **2002**, *27*, 469.
(41) Liao, Z.-R.; Zheng, X.-F.; Luo, B.-S.; Shen, L.-R.; Li, D.-F.; Liu, H.-L.; Zhao, W. *Polyhedron* **2001**, *20*, 2813.
(42) Viossat, V.; Lemoine, P.; Dayan, E.; Dung, N.-H.; Voissat, B. *Polyhedron* **2003**, *22*, 1461.
(43) Oki, A. R.; Gogineni, P.; Yurchenko, M.; Young, V. G., Jr *Inorg. Chim. Acta* **1997**, *257*, 279.
(44) Baldeau, S. M.; Slinn, C. H.; Krebs, B.; Rompel, A. *Inorg. Chim. Acta* **2004**, *357*, 3295.
(45) Platas-Iglesias, C.; Vaiana, L.; Esteban-Gómez, David.; Avecilla, F.; Real, J. A.; Blas, A. de; Rodríguez-Blas, T. *Inorg. Chem.* **2005**, *44*, 9704.
(46) Ghachtouli, S. E.; Mohamadou, A.; Barbier, J.-P. *Inorg. Chim. Acta* **2005**, *358*, 3873.
(47) Coronado, E.; Galán-Mascarós, J. R.; Martí-Gastaldo, C.; Martínez, A. M. *Dalton Trans.* **2006**, 3294.

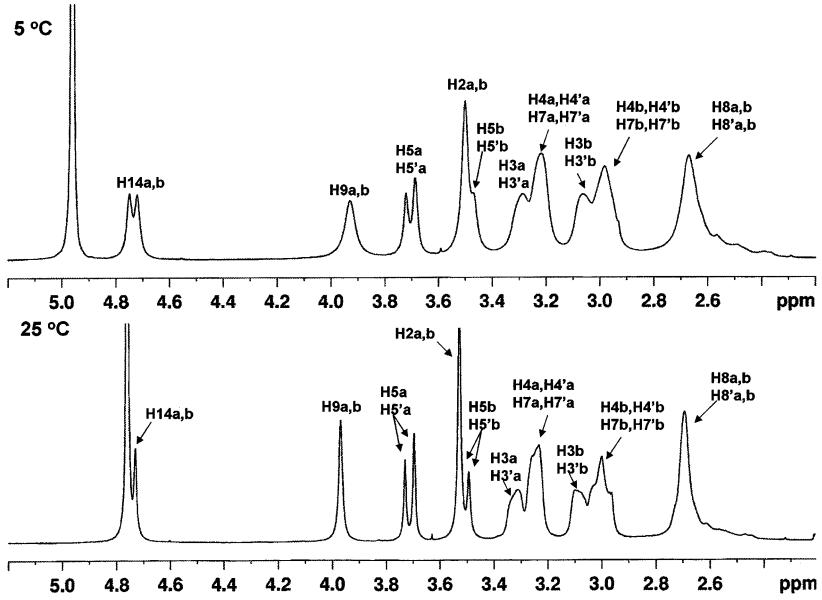


**Figure 7.** Aliphatic region of the $^1$H NMR spectra of In(DO3A-xy-TPP)$^+$ in $D_2O$ at 5 (top) and 25 °C (bottom).

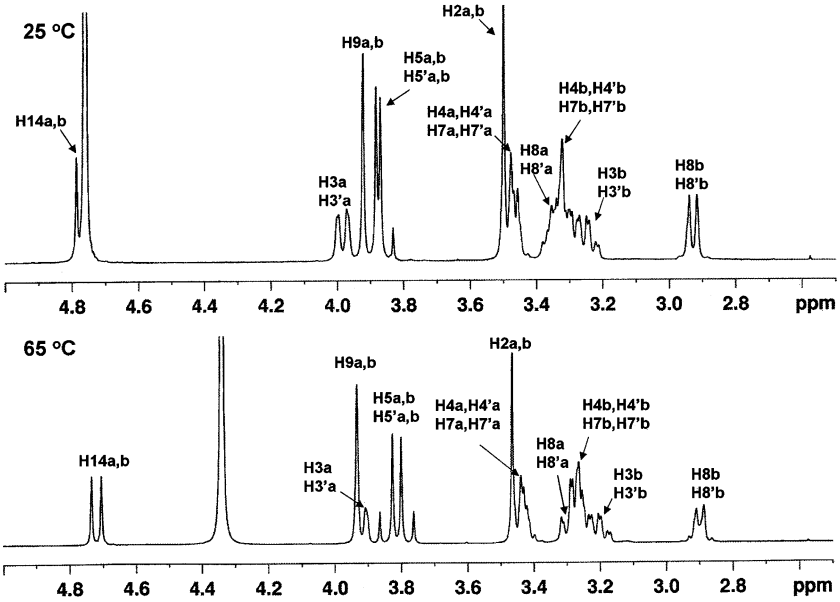


**Figure 8.** Aliphatic region of the $^1$H NMR spectra of Ga(DO3A-xy-TPP)$^+$ in $D_2O$ at 25 (top) and 65 °C (bottom).

H8a′, H8b, and H8b′) of the cyclen macrocycle. As the temperature increases from 5 to 25 °C, all signals become sharper with no significant change in their chemical shifts.

Figure 8 shows the aliphatic region of $^1$H NMR spectra of Ga(DO3A-xy-TPP)$^+$ in $D_2O$ at 25 (top) and 65 °C (bottom). The doublet at 4.78 ppm is assigned to H14 and H14′ of the P*CH*$_2$C$_6$H$_4$ moiety. The singlet at 3.92 ppm is from H9 and H9′ of the N*CH*$_2$C$_6$H$_4$ moiety. The singlet at 3.49 is assigned to methylene protons (H2a and H2b) in the uncoordinated acetate group. The AB quartet at ~3.85 ppm are from four methylene protons (H5a and H5′) in the two opposite acetate chelating arms due to the asymmetric nature of Ga(DO3A-xy-TPP)$^+$. The multiplets at 4.02 and 3.26 ppm are tentatively assigned to methylene protons (H3a, H3a′, H3b, and H3b′) of the cyclen macrocycle. The multiplets at 3.35 and 3.51 ppm are from eight methylene protons (H4, H4′, H7, and H7′) and the multiplets at 2.89 and 3.39 ppm are from remaining four methylene protons (H8a, H8a′, H8b, and H8b′) on the macrocyclic framework. As the temperature increases from 25 to 65 °C, all proton resonance signals remain the same, except for the multiplet at 4.0 ppm, which shifted to 3.9 ppm probably because of rapid inversion of ethylenic groups on the cyclen macrocycle.

## Discussion

This report describes synthesis and structural characterization of Ga(DO3A-xy-TPP)$^+$, In(DO3A-xy-TPP)$^+$, and Mn-(DO3A-xy-TPP). The most important finding from this study is that the bonding mode of DO3A depends largely on the size of metal ion. For example, the ionic radius of In(III) is 0.92 Å,[48] and DO3A is heptadentate in In(DO3A-xy-TPP)$^+$. Mn(II) has an ionic radius of 0.90 Å, and the coordination

(48) Shannon, R. D. *Acta Crystallogr.* **1976**, *A32*, 751.

geometry around Mn(II) in Mn(DO3A-xy-TPP) is almost identical to that in In(DO3A-xy-TPP)$^+$, despite their charge difference. Ga(III) has a much smaller ionic radius (0.62 Å).[48] As a result, coordinated DO3A is hexadentate with one acetate group remaining deprotonated in Ga(DO3A-xy-TPP)$^+$. The overall molecular charge of Ga(DO3A-xy-TPP)$^+$ is the same as that of In(DO3A-xy-TPP)$^+$.

The solution structure of In(DO3A-xy-TPP)$^+$ and Ga(DO3A-xy-TPP)$^+$ is important for understanding the coordination chemistry of DO3A-conjugated TPP cations with $^{67/68}$Ga and $^{111}$In at the tracer level. On the basis of HPLC concordance experiments, it is concluded that $^{111}$In(DO3A-xy-TPP)$^+$ and In(DO3A-xy-TPP)$^+$ have the same composition because of their identical HPLC retention times (Figure 3). In(DO3A-xy-TPP)$^+$ remains symmetrical in aqueous solution. This conclusion is supported by the fact that the proton resonance signals from the N*CH*$_2$C$_6$H$_4$ moiety and the acetate arm attached to N(7) appear as two singlets at 3.96 and 3.53 ppm, respectively. The presence of the AB quartet at ∼3.62 ppm clearly indicates that all three carboxylate-O donors are firmly bonded to In(III). If these carboxylate-O donors were dissociated, there would have been three singlets: one from the central acetate group, one from the N*CH*$_2$C$_6$H$_4$ moiety, and one from the two remaining acetate arms.

This symmetrical structure Ga(DO3A-xy-TPP)$^+$ is also maintained in solution as evidenced by the presence of two singlets at 3.92 and 3.54 ppm from the N*CH*$_2$C$_6$H$_4$ moiety and the acetate arm attached to N(7), respectively. Since the two methylene hydrogens of the coordinated acetate chelating arms experience different chemical environments, it is not surprising that they appear as the AB quartet at ∼3.65 ppm. The two coordinated carboxylate-O donor atoms remain firmly bonded to Ga(III) even at 65 °C (Figure 4), suggesting that $^{68}$Ga(DO3A-xy-TPP)$^+$ might have a very high in vivo solution stability as observed for $^{68}$Ga(DOTA-D-Phe-NH$_2$)$^+$.[37]

Comparison of the $^1$H NMR spectra (Figures 7 and 8) of In(DO3A-xy-TPP)$^+$ and Ga(DO3A-xy-TPP)$^+$ reveals certain similarities in the splitting patterns for H2, H5, H9, and H14, as well as significant differences in chemical shifts of H3, H4, H7, and H8. The fact that both H3a and H8a have significantly different chemical shifts (Table 1) in the $^1$H NMR spectra of In(DO3A-xy-TPP)$^+$ and Ga(DO3A-xy-TPP)$^+$ strongly suggests that they might have different solution structures as those observed in the solid state (Figures 4 and 5). It is important to note that the most common coordination number for In(III) is 6 or 7, while the coordination number of Ga(III) is predominantly 6 because of its smaller ionic radius.[34,35,38,39,48] Therefore, it is reasonable to believe that the solution structure of Ga(DO3A-xy-TPP)$^+$ is the same as that in the solid state (Figure 5) with one acetate chelating arm being uncoordinated.

## Conclusion

In conclusion, Ga(DO3A-xy-TPP)$^+$, In(DO3A-xy-TPP)$^+$, and Mn(DO3A-xy-TPP) have been prepared and characterized by elemental analysis, spectroscopic methods, and X-ray crystallography. In the solid state, DO3A uses all of its seven donor atoms ($N_4O_3$) in bonding to In(III) or Mn(II), while it is only hexadentate in bonding to Ga(III) with four amine-N and only two carboxylate-O donor atoms. The NMR data clearly demonstrate that the coordinated DO3A in In(DO3A-xy-TPP)$^+$ and Ga(DO3A-xy-TPP)$^+$ is symmetrical in aqueous solution. The variable-temperature $^1$H NMR data reveal no dissociation of the two acetate chelating arms in Ga(DO3A-xy-TPP)$^+$, which remains rigid in aqueous solution even at temperatures over 65 °C.

Another important finding from this study is that Ga(DO3A-xy-TPP)$^+$ and In(DO3A-xy-TPP)$^+$ are more hydrophilic than Mn(DO3A-xy-TPP), the HPLC retention time of which is very close to that of Cu(DO3A-xy-TPP).[26] This suggests that Cu(DO3A-xy-TPP) may also exist in solution as its zwitterion form as observed in Mn(DO3A-xy-TPP), despite their difference in coordination number resulting from the smaller ionic radius of Cu(II) (0.67 Å) than Mn(II) (0.90 Å).[48] Because the ionic radius of Cu(II) is very close to that of Ga(III) (0.62 Å),[48] we believe that the coordinated DO3A in Cu(DO3A-xy-TPP) is most likely hexadentate with one acetate group being deprotonated to balance to cationic charge from the TPP moiety. Evaluation of radiometal chelate and overall molecular charge on biological properties of the radiolabeled TPP cation is still in progress, and the results from these studies will be reported elsewhere.

**Acknowledgment.** Acknowledgement is made to Dr. Huaping Mo for his help with NMR data analysis and to Dr. Philip E. Fanwick, Department of Chemistry, Purdue University, for X-ray crystallography of In(DO3A-xy-TPP)(OAc)·7.5H$_2$O·(CH$_3$)$_2$CO, Ga(DO3A-xy-TPP)(NO$_3$)·6H$_2$O·(CH$_3$)$_2$CO, and Mn(DO3A-xy-TPP)·4H$_2$O·CH$_3$OH. This work is supported, in part, by Purdue University and research grants (1R01 CA115883-01A2 (S.L.)) from National Cancer Institute (NCI), (BCTR0503947 (S.L.)) the Susan G. Komen Breast Cancer Foundation, (AHA0555659Z (S.L.)) the Greater Midwest Affiliate of American Heart Association, (R21 EB003419-02 (S.L.)) National Institute of Biomedical Imaging and Bioengineering (NIBIB), and (R21 HL083961-01) National Heart, Lung, and Blood Institute (NHLBI).

**Supporting Information Available:** X-ray crystallographic files are in CIF format for the reported structures In(DO3A-xy-TPP)(OAc)·7.5H$_2$O·(CH$_3$)$_2$CO, Ga(DO3A-xy-TPP)(NO$_3$)·6H$_2$O·(CH$_3$)$_2$CO, and Mn(DO3A-xy-TPP)·4H$_2$O·CH$_3$OH and 2D NMR spectra for In(DO3A-xy-TPP)$^+$ and Ga(DO3A-xy-TPP)$^+$. This material is available free of charge via the Internet at http://pubs.acs.org.

IC7010452